Research Article

GAZİ
JOURNAL OF ENGINEERING SCIENCES

# Experimental Investigation of the Machinability of Basalt Fiber Reinforced Epoxy Matrix Composites and the Effect of Nanoparticle Additives on Machining Quality

**Mehmet Tongur**[*a], **Necati Ataberk**[b]
**Submitted:** 06.05.2024 **Revised:**16.07.2025 **Accepted:** 18.08.2025 **doi:**10.30855/gmbd.070525A11

[a,*] Necmettin Erbakan University Engineering and Architectural Faculty, Mechanical Engineering Department, Konya, Türkiye, Orcid: 0000-0002-5847-3295
[b] Necmettin Erbakan University Engineering and Architectural Faculty, Mechanical Engineering Department, Konya, Türkiye, Orcid: 0000-0002-5394-9549
*Corresponding author: mehmettongur@ahievran.edu.tr*

**Keywords:**
Basalt fiber fabric, MWCNT nanoparticles, delamination damage, hexagonal boron nitride nanoparticles, surface roughness, drilling

## ABSTRACT

In this study, basalt fiber-reinforced epoxy matrix composite materials were produced using hand lay-up and vacuum infusion methods, both in their unreinforced form and with the addition of 0.25 wt% multi-wallet carbon nanotube (MWCNT) and 0.5 wt% hexagonal boron nitride (h-BN) nanoparticles. Additionally, hybrid basalt fiber-reinforced epoxy matrix composites were manufactured by keeping the MWCNT content constant at 0.25 wt% while varying the h-BN reinforcement levels to 0.25 wt%, 0.5 wt%, and 0.75 wt%. The effects of nanoparticle reinforcement, cutting speed, and feed rate on parameters such as cutting force, delamination, and average surface roughness ($R_a$) during drilling processes were investigated. Among the cutting forces observed, the lowest thrust forces during drilling were achieved for all samples at a feed rate of 300 mm/min and a spindle speed of 4800 rpm. When comparing reinforcement levels, the lowest cutting force values were obtained in sample N5, which contained the highest h-BN nanoparticle reinforcement. In terms of surface roughness, the lowest value of 0.95 µm was achieved for sample N5 at a feed rate of 300 mm/min and a spindle speed of 4800 rpm during the drilling process. Regarding delamination, it was observed that increasing h-BN content, combined with low feed rates and high spindle speeds, reduced delamination damage in drilling processes

## 1. Introduction

Composite materials have found widespread use in aerospace, automotive, and other engineering fields due to their superior mechanical properties, lightweight nature, and resistance to corrosion. These characteristics make them a strong alternative to metal alloys in many engineering applications [1]. Various fibers such as basalt, glass, jute, flax, aramid, and carbon fibers are used as reinforcement materials in composites [2]. Among these, basalt fiber stands out as an important reinforcement in polymer matrix composites due to its non-toxic nature, eco-friendliness, ease of processing, and cost-effectiveness compared to other fibers [3]. Composite materials are generally produced using molding techniques, but secondary operations such as drilling, milling, and surface finishing are required for assembly and dimensional tolerances [4]. During these machining processes, defects such as fiber breakage, resin separation, micro-cracks, and delamination may occur due to the anisotropic and heterogeneous structure of composites [5]. To reduce these defects, adding specific amounts of nanoparticles to the composites has proven to be an effective solution [6]. Nanoparticles such as boron nitride graphene, MWCNTs, and fullerenes enhance the machinability of composites while significantly improving the wear resistance of the matrix. MWCNTs, with their high surface area, exceptional tensile strength (up to 60 GPa), and elasticity modulus (approximately 1 TPa), are prominent as fillers in composites. Additionally, lubricants like hexagonal boron nitride and boric acid provide slipperiness due to weak Van der Waals bonds between their layers, improving wear performance. Boron nitride, in particular, is widely used in composite materials and advanced technological

**To cite this article**: M. Tongur and N. Ataberk "Experimental Investigation of the Machinability of Basalt Fiber Reinforced Epoxy Matrix Composites and the Effect of Nanoparticle Additives on Machining Quality," Gazi Journal of Engineering Sciences, vol.11, no.2, pp. 274-290, 2025. doi:10.30855/gmbd.070525A11

applications to enhance wear resistance, reduce friction, and improve thermal management. In conclusion, nanoparticle reinforcement not only strengthens the mechanical properties of composites but also reduces machining-related defects, thereby improving the overall performance of the material [7]. Composite materials are widely used in the aerospace and aviation industries, where drills with a diameter of 4.8–10 mm and a point angle of 110–140º are generally preferred for drilling operations [7-10]. In terms of cutting tool materials, the abrasive properties of fiber-reinforced composites result in lower performance for HSS (High-Speed Steel) tools. Therefore, WC (Tungsten Carbide) tools emerge as a more efficient alternative [11]. Additionally, studies in the literature highlight the superior performance of diamond-coated tools, particularly in wear resistance tests [12-13]. Tungsten carbide drill bits outperform HSS drill bits significantly. The main reasons for this superiority are the excellent thermal stability of carbide tools at high temperatures, their ability to maintain hardness, and their excellent wear resistance [14-15]. As a result of the literature review, it has been observed that studies on the machinability of basalt fiber-reinforced epoxy matrix composites are quite limited. In particular, the lack of information on nanoparticle-reinforced composites containing h-BN and MWCNT highlights the need for more in-depth research in this field. In this study, the machinability of both unreinforced and nanoparticle-reinforced basalt fiber composites was examined in detail with the aim of addressing this knowledge gap and revealing their potential for industrial applications. During the drilling process, the effects of machining parameters such as cutting speed and feed rate on key output parameters—cutting force, delamination, and surface roughness were systematically evaluated. The findings are expected to contribute to the improvement of production processes involving advanced composites and to provide valuable guidance for both academic research and industrial practices.

## 2. Materials and Method

### 2.1. Materials

In this study, the composite material produced with epoxy resin nanoparticle reinforcement was used as a matrix element. The epoxy resin (LR160) and hardener (LH160) utilized in the study were supplied by Dost Kimya. Additionally, the basalt fabric used as a reinforcement element was a 200 g/m$^2$ plain weave basalt fiber fabric, procured from Kompozitsan company. MWCNTs and h-BN were employed as nanoparticles. The MWCNTs used have an outer diameter ranging from 15 to 25 µm, an inner diameter of 5 to 10 µm, and lengths varying between 10 and 20 µm. The h-BN nanoparticles have a purity of 99.5% and a diameter of 65-75 µm. These nanoparticles were supplied by Nanografi company. In this study, a TiAlN-coated carbide drill bit with a diameter of 6 mm, supplied by TAEGUTEC, was used for the drilling process (Figure 1).

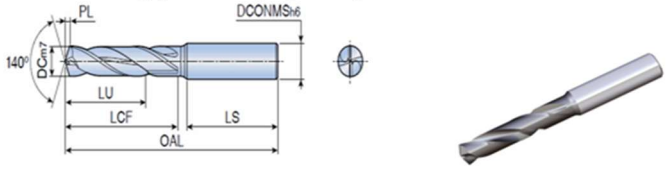


| DC | DCONMS | OAL | LU | LCF | LS | PL |
|---|---|---|---|---|---|---|
| 6.00 | 6.00 | 66.00 | 20.0 | 29.000 | 36.0 | 0.9 |

Figure 1. Dimensions and properties of the TiAlN-coated ca

### 2.2. Preparation of nanoparticles doped epoxy resin

According to literature research, the ratios of h-BN and CNT nanoparticle additives in matrix elements have been determined to not exceed a total of 1%. The best mechanical properties for CNT addition were found at 0.25% [16-18], and for h-BN, the optimal ratio was 0.50% [19]. In this study, nanoparticle-reinforced epoxy resins were initially prepared with 0.25 wt.% MWCNT nanoparticle content and 0.5 wt.% h-BN reinforcement. Subsequently, hybrid nano-epoxy resins were developed by maintaining the MWCNT content at a constant 0.25 wt.% and varying the h-BN reinforcement at 0.25 wt.%, 0.5 wt.%, and 0.75 wt.%, enabling the investigation of the effects of h-BN nanoparticle reinforcement within the matrix. In other words, this approach aimed to observe improvements in cutting performance by leveraging the superior mechanical properties of MWCNTs and the exceptional lubricating properties of h-BN nanoparticles. In the solution mixing method, clean epoxy resin was placed into an empty beaker using a precision scale, and nanoparticles in varying weight percentages, as detailed in Table 1, were added based on the epoxy resin quantity. The mixture was homogenized using a Bandelin HD 2200 ultrasonic mixer

ISSN: 2149-9373 

operating at 20 kHz and 70 W for 5 minutes. To prevent excessive heating that could compromise the structure of the epoxy and nanoparticles, intermittent temperature measurements were taken, and cooling was applied as necessary. Subsequently, a curing agent at 25 wt.% of the epoxy resin's weight was added to the mixture and stirred for 5 minutes using a mechanical stirrer until a homogeneous mixture was achieved. The nanoparticle-reinforced epoxy resins were thus prepared for composite material production (Figure 2).

Table 1.Naming of the produced nanocomposite materials

| Samples | Additive by Weight (gr) | MWCNT(%) | h-BN (%) |
|---|---|---|---|
| N0 | Neat Epoxy | 0 | 0 |
| N1 | Epoxy +%0.5 h-BN | 0 | 0.5 |
| N2 | Epoxy+%0.25 MWCNT | 0.25 | 0 |
| N3 | Epoxy+%0.25 MWCNT +% 0.25h- | 0.25 | 0.25 |
| N4 | Epoxy+%0.25 MWCNT +% 0.50h- | 0.25 | 0.5 |
| N5 | Epoxy +%0.25 MWCNT +% 0.75h- | 0.25 | 0.75 |

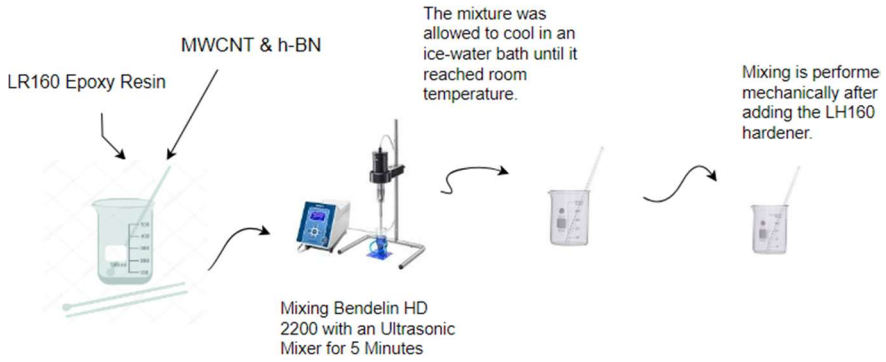


Figure 2. Preparation of epoxy resin with nanoparticle additives.

## 2.3. Production of composite plates

The production of composite materials was carried out by simultaneously using two production methods, hand lay-up + vacuum bagging. During the production phase, an epoxy + hardener mixture containing nanoparticles was impregnated into 16 layers of basalt fabric using a roller brush, ensuring the homogeneous distribution of the nanoparticles. Subsequently, the vacuum bagging method was applied to eliminate air pockets (Figure 3). According to the epoxy resin catalog data, the mixture was heated and left to cure. A stepwise heating process was applied during curing: 10 minutes at 50ºC, 120 minutes at 80ºC, and 120 minutes at 120ºC. Afterward, the material was left to cool at room temperature. The reason for keeping the temperature low during the initial curing stage is to prevent the chemical structure of the uncured epoxy from being degraded by high temperatures [20]. Then, the vacuum tape, nylon, infusion mesh, and peel ply were removed, and the excess edges of the composite plates were trimmed using a circular saw. In total, six 300x300x4.75±0.25 mm and 30x30 mm plates, one from each mixture ratio, were obtained to be used in the drilling process.


Figure 3. Production of composite plates using hand lay-up + vacuum bagging method

## 2.4. Characterization

The experiments were conducted on the Quaser MV154C vertical machining center, which is shown in Figure 4 and Figure 5, with a maximum power of 17.5 kW and a spindle speed of 10,000 rpm. A special mold was designed for drilling operations and the mold was mounted on a dynamometer for cutting force measurements. The thrust force was measured using the Kistler 9257B dynamometer, fixed to the machine, along with the 5070A amplifier, 5697A data acquisition unit, and DynoWare software, at a sampling rate of 2000 Hz. After the measurements, raw force-time data was obtained, and the maximum force data throughout the process was recorded. Thrust forces were measured for all parameters tested in the experiments. During drilling, a mold was produced to mount the Kistler 9257B dynamometer, and composite plates were attached to the upper part of the mold using specially made pads. Drilling was carried out with five repetitions for each parameter, ensuring that the plate was fully perforated. Since the cutting force components in the x ($F_x$) and y ($F_y$) directions were very low during the drilling process, the cutting force in the z direction ($F_z$), referred to as the thrust force, was used for machinability evaluation [21].

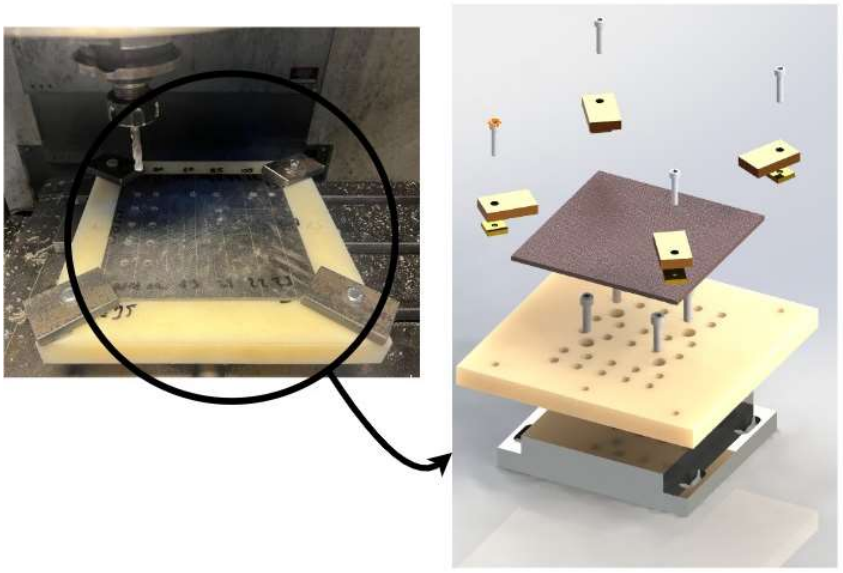

Figure 4. The drilling operations were performed on a CNC vertical machining center, utilizing a mold specifically designed for drilling and a dynamometer assembly for force measurement.

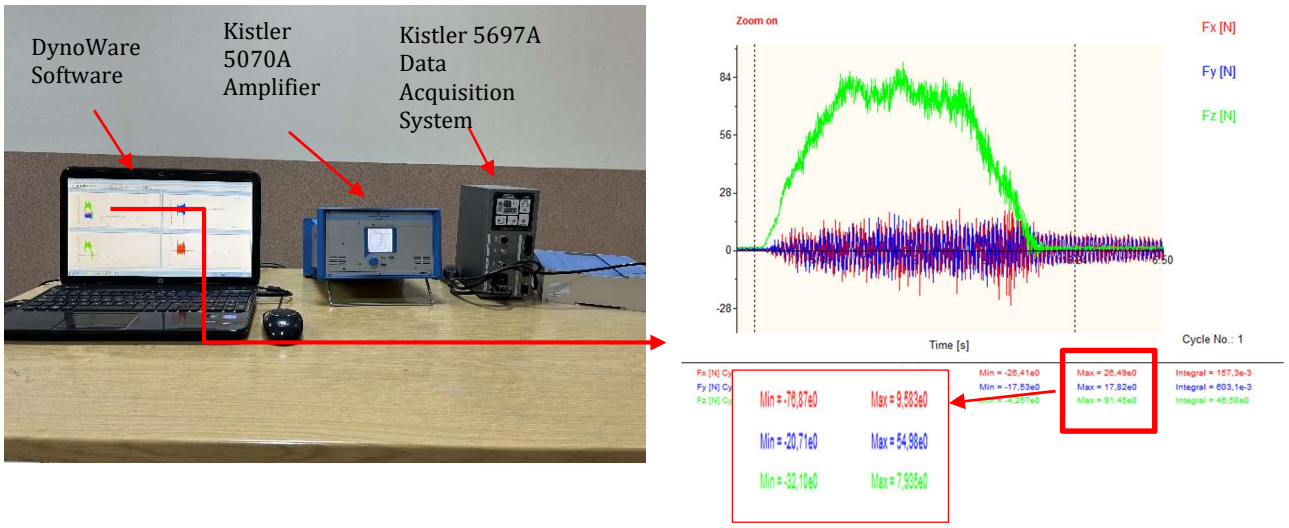


Figure 5. The equipment used for cutting force measurements (Dynoware software, amplifier and data acquisition system, maximum forces generated during the drilling process)

The process parameters were determined based on N: spindle speed (rpm), Vc: cutting speed (m/min), D: tool diameter (mm), F: feed rate (mm/min) and fz: feed per rpm (mm/rpm). For the machining of composite materials, the cutting speed (30-90 m/min) and feed rate (0.18 mm/tooth) values taken from the company catalog were substituted into Equations 1 and 2 [22] to calculate the spindle speed and feed rate. As a result, 6 mm diameter drill, cutting speeds of L1: 300 mm/min and L2: 800 mm/min, and spindle speeds of S1: 1600 rpm, S2: 3200 rpm, and S3: 4800 rpm were determined. While calculating the spindle speed, an intermediate value was also selected in addition to the two main values in order to enhance the accuracy of the study. This approach allowed for more reliable results and enabled a more comprehensive evaluation. The obtained values were presented in Table 2.

$$N = \frac{1000.V_c}{\pi.D} \tag{1}$$

$$F = f_z.N \tag{2}$$

Table 2.The cutting parameters calculated for the drilling operation

| Tool Diameter (mm) | Cutting Speed Vc (m/min) | Feed Rate (mm/rpm) | Feed Rate (mm/min) | Spindle Speed (rpm/min) |
|---|---|---|---|---|
| 6 | 30 | 0.18 | 299.36 | 1592.35 |
| 6 | 90 | 0.18 | 878.98 | 4777.07 |

After the drilling operation, the images of the entry and exit sections of each hole for each experimental parameter were captured and recorded using the Keyence VHX-900F digital microscope. Then, in AutoCAD software[23], the nominal hole diameter and the diameter measurements of the maximum delaminated area were determined. The delamination factor (Fd), which characterizes the delamination level, was calculated by taking the ratio of the diameter of the circle containing the maximum damaged area ($D_{max}$) to the nominal hole diameter ($D_{nom}$), as shown in Equation 3 [24]. The stages of examining and calculating delamination damage were shown in Figure 6.

$$F_d = \frac{D_{\max}}{D_{\text{nom}}} \tag{3}$$

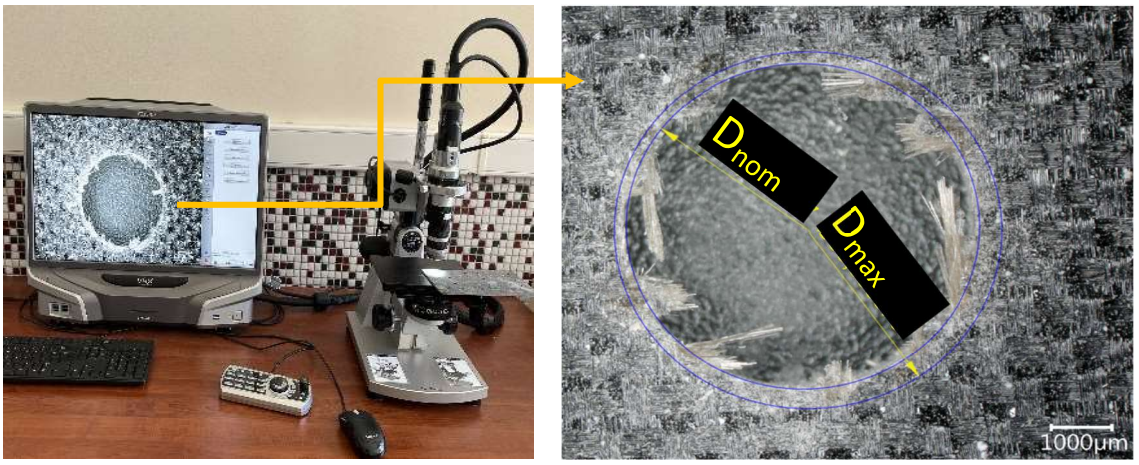


Figure 6. The stages of delamination damage measurement

In drilling operations, surface roughness was measured at a single point on the hole surfaces. All surface measurements were performed using the FILMETRICS Profilm3D-200 optical profilometer, and the measurements were analyzed using Profilmonline software. The experimental setup used is shown in Figure 7.

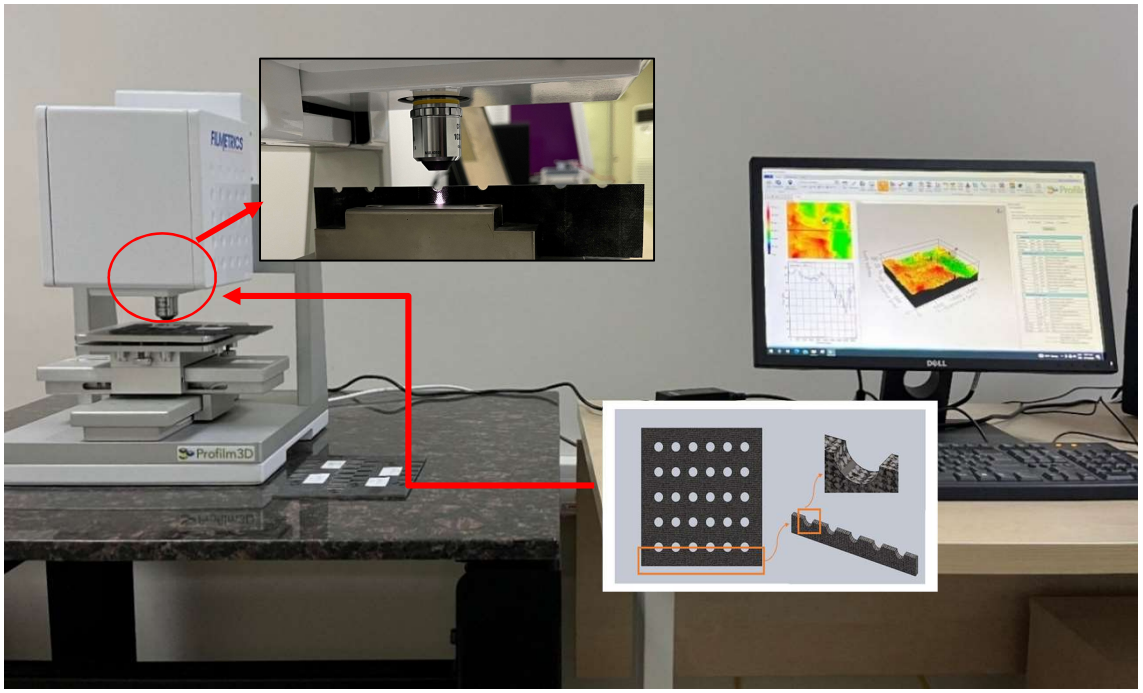


Figure 7. Surface roughness measurement using the FILMETRICS Profilm3D-200 optical profilometer and Profilmonline software

## 3. Results and Discussion

### 3.1. Test results for thrust force analysis in drilling operation

Thrust force measurements were completed with five repetitions for each parameter combination. The results obtained from the measurements, including the percentage changes of samples N1, N2, N3, N4, and N5 compared to the N0 sample, were collectively presented in Table 3. The thrust force values determined based on contribution rates were provided in Figure 8.

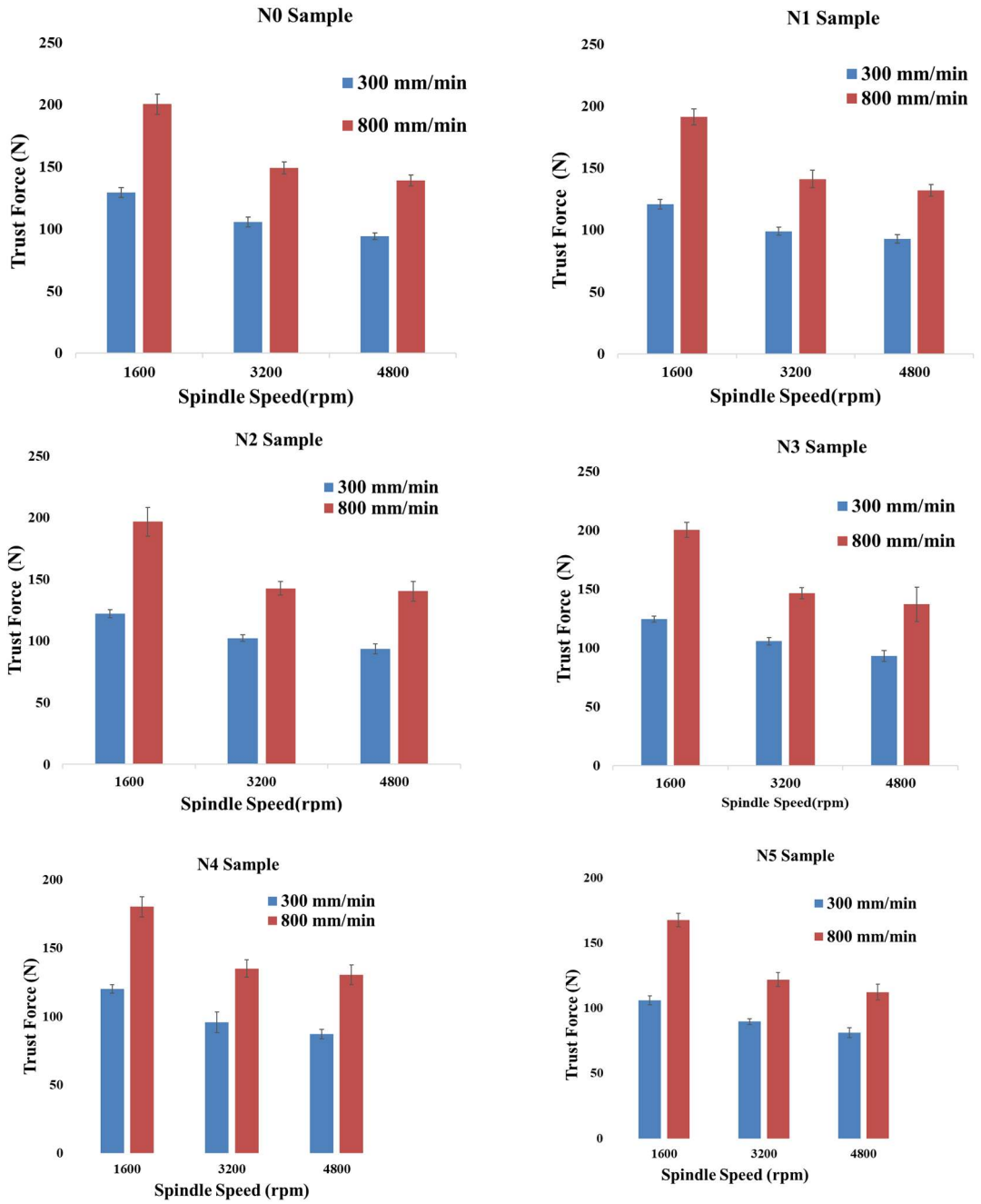


Figure 8. Maximum thrust forces generated in the Z-direction for N0, N1, N2, N3, N4, and N5 samples.

Table 3.Maximum $F_z$ thrust force values generated in the Z-direction during the drilling process for N0, N1, N2, N3, N4, and N5 samples.

| Samples | $F_z$ Trust Force (N) | Percentage change rates (%) |
|---|---|---|
| dN0-L1-S1 | 129.4±3.91 | - |
| dN0-L1-S2 | 105.6±4.14 | - |
| dN0-L1-S3 | 94.19±2.83 | - |
| dN0-L2-S1 | 200.4±8.13 | - |
| dN0-L2-S2 | 149.1±4.96 | - |
| dN0-L2-S3 | 139.2±4.36 | - |

| Samples | $F_z$ Trust Force (N) | Percentage change rates (%). |
|---|---|---|
| dN1-L1-S1 | 120.70±3.82 | -6.72 |
| dN1-L1-S2 | 98.99±3.28 | -6.26 |
| dN1-L1-S3 | 92.76±3.49 | -1.51 |
| dN1-L2-S1 | 191.5±6.47 | -4.44 |
| dN1-L2-S2 | 141.28±6.91 | -5.24 |
| dN1-L2-S3 | 132.11±4.84 | -5.17 |

| Samples | $F_z$ Trust Force (N) | Percentage change rates (%). |
|---|---|---|
| dN3-L1-S1 | 124.8±3.15 | -3.55 |
| dN3-L1-S2 | 105.85±7.66 | 0.24 |
| dN3-L1-S3 | 93.25±3.37 | -0.99 |
| dN3-L2-S1 | 200.32±7.35 | -0.04 |
| dN3-L2-S2 | 146.8±6.52 | -1.54 |
| dN3-L2-S3 | 137.24±7.15 | -1.41 |

| Samples | $F_z$ Trust Force (N) | Percentage change rates (%) |
|---|---|---|
| dN2-L1-S1 | 122.08±3.34 | -6.00 |
| dN2-L1-S2 | 102.318±2.71 | -3.21 |
| dN2-L1-S3 | 93.51±4.04 | -0.73 |
| dN2-L2-S1 | 196.65±11.6 | -1.91 |
| dN2-L2-S2 | 142.7±5.35 | -4.48 |
| dN2-L2-S3 | 140.02±7.97 | 0.78 |

| Samples | $F_z$ Trust Force (N) | Percentage change rates (%). |
|---|---|---|
| dN4-L1-S1 | 120.02±2.52 | -7.25 |
| dN4-L1-S2 | 95.61±3.22 | -9.46 |
| dN4-L1-S3 | 87.08±4.63 | -7.55 |
| dN4-L2-S1 | 180.36±6.39 | -10.00 |
| dN4-L2-S2 | 135.1±4.71 | -9.39 |
| dN4-L2-S3 | 130.42±14.61 | -6.31 |

| Samples | $F_z$ Trust Force (N) | Percentage change rates (%) |
|---|---|---|
| dN5-L1-S1 | 105.9±3.48 | -18.16 |
| dN5-L1-S2 | 89.638±2.26 | -15.12 |
| dN5-L1-S3 | 81.082±3.77 | -13.92 |
| dN5-L2-S1 | 167.52±5.09 | -16.41 |
| dN5-L2-S2 | 121.94±5.42 | -18.22 |
| dN5-L2-S3 | 112.3±5.95 | -19.32 |

Thrust force is critically important for understanding potential severe damage during the drilling process of composite materials. It serves as an indicator of cutting tool performance, with variations in thrust force often stemming from drill wear and changes in the material removal mechanism. Increased feed rates lead to greater contact between the drill tips and the work piece, thereby increasing thrust force. Conversely, higher spindle speeds reduce thrust force. The findings reveal that the most influential factor on thrust force is the feed rate, followed by spindle speed as a secondary factor. An increase in feed rate enhances contact between the work piece and the cutting tool, resulting in higher thrust forces. However, higher speeds cause chips to remain in the cutting zone for a shorter duration [25], which contributes to the reduction of thrust force at a feed rate of 300 mm/min. On the other hand, when the feed rate reaches 800 mm/min, the reduced contact time between the drill bit and the work piece diminishes the polishing effect, leading to a rise in thrust force again [26]. These results underscore the importance of accurately optimizing parameters such as feed rate and spindle speed to minimize thrust force-induced damage during drilling. The lowest thrust force, 81.08 N, was observed in the dN5-L1-S3 sample at a feed rate of 300 mm/min and a spindle speed of 4800 rpm. Across all samples, the lowest thrust forces were recorded at the L1-S3 levels, corresponding to a feed rate of 300 mm/min and a spindle speed of 4800 rpm. This indicates that low feed rates combined with high spindle speeds reduce contact between the cutting tool and the work piece, minimizing thrust force. Thrust force is largely controlled by the cutting mechanism during machining. Excessive MWCNT reinforcement can alter the chip removal mechanism by shifting the cutting process from the polymer matrix to the MWCNTs during drilling [27]. This resulted in higher thrust forces in the N2 sample compared to the N1, N3, N4, and N5 samples. While higher MWCNT ratios improve machinability up to a certain threshold by lowering thrust force, exceeding this threshold negatively impacts machinability [28]. The h-BN additive, by weight, reduces thrust force due to its friction-reducing properties and lubricating effect [29]. Therefore, lower thrust forces were achieved with increasing h-BN additive ratios. In the MWCNT-reinforced N2 sample, the added MWCNT by weight reduced thrust force, but the reduction was less significant compared to the h-BN-reinforced N1, N3, N4, and N5 samples. In other words, while the MWCNT additive positively impacted strength properties, it negatively affected thrust force. In contrast, the h-BN nanoparticle additive by weight had a more positive effect on thrust force compared to the MWCNT additive, while also modifying the strength properties.

ISSN: 2149-9373 

### 3.2. Test results for delamination analysis in drilling operation

After the drilling process, the entry and exit areas of each hole were imaged using the Keyence VHX-900F digital microscope. The images of the samples N0, N1, N2, N3, N4, and N5 were provided sequentially in Figure 9, Figure 10, Figure 11, Figure 12, Figure 13 and Figure 14. The delamination factor measurements for all samples were summarized in Table 4, Figure 15 and Figure 16.

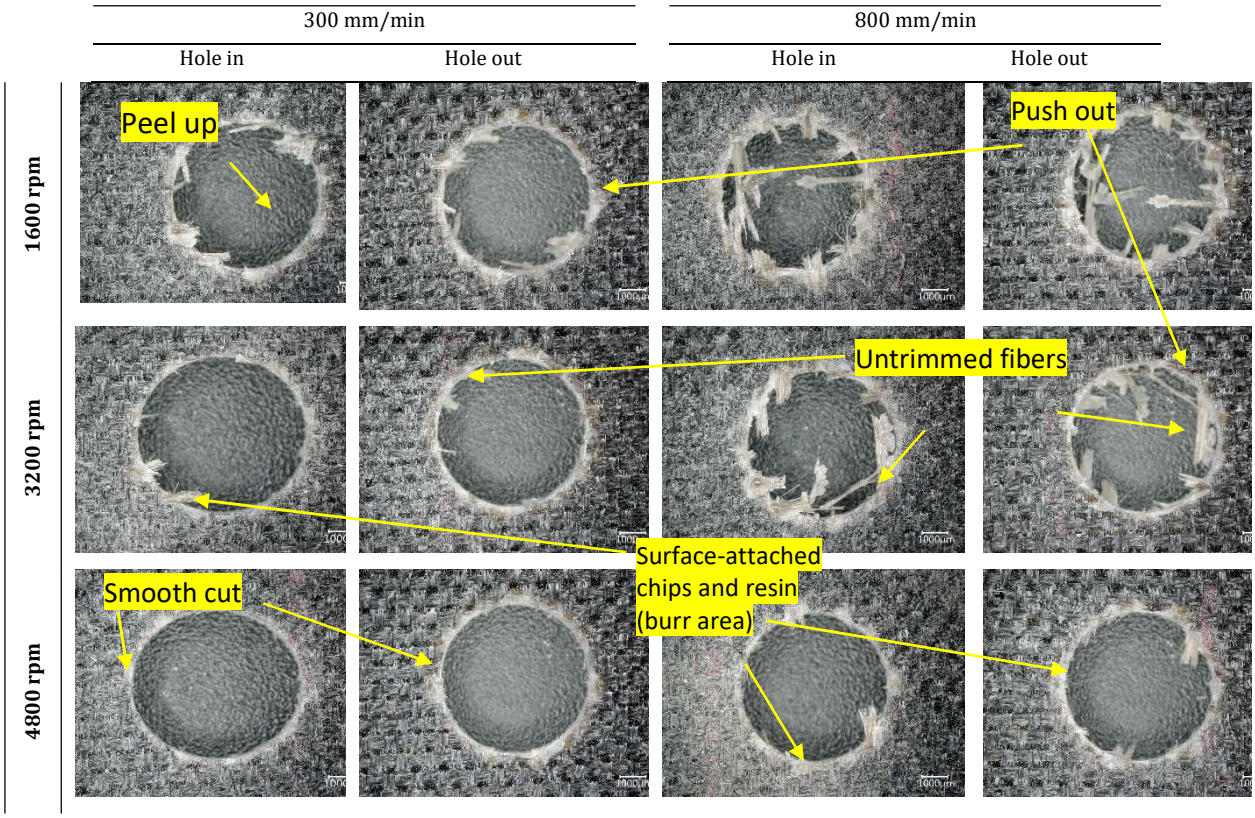


Figure 9. Microscope images of the hole in and out for the N0 sample

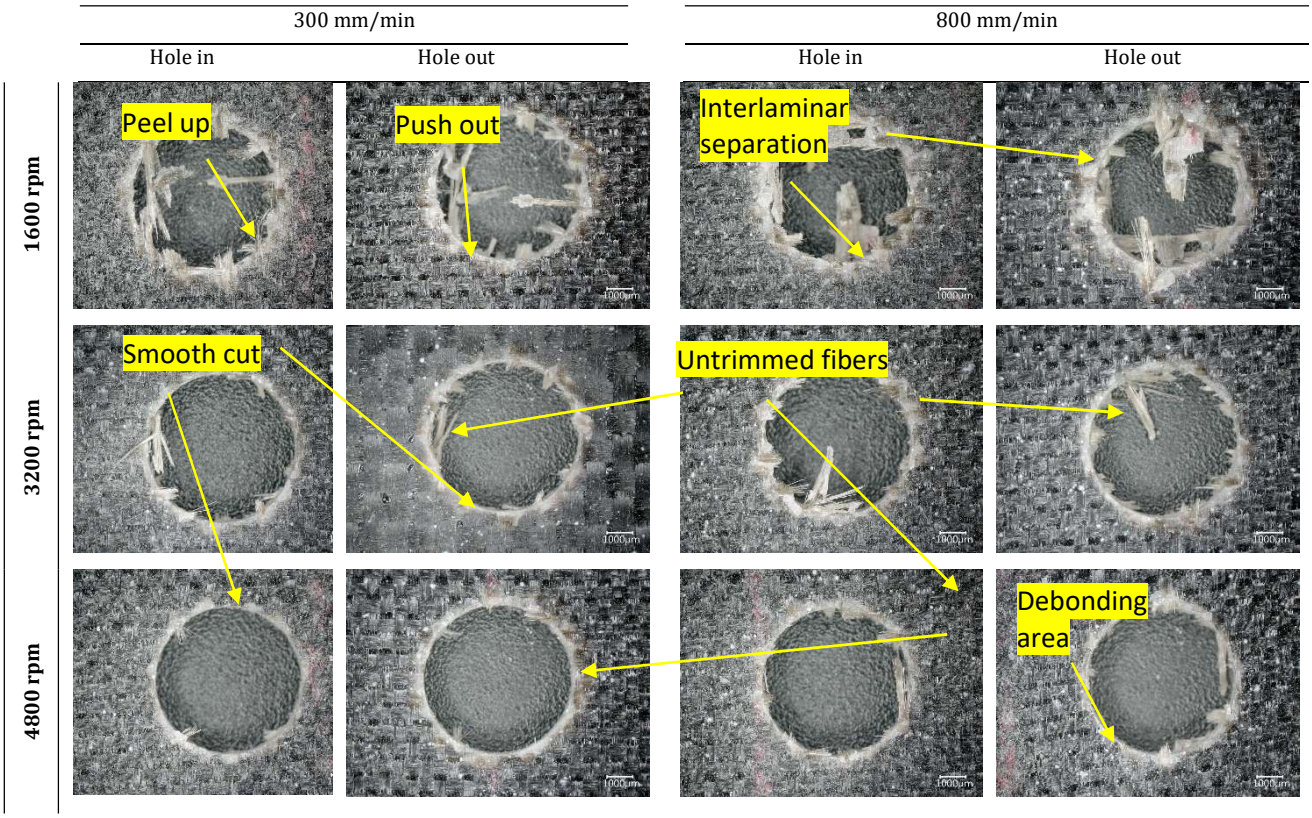


Figure 10. Microscope images of the hole in and out for the N1 sample

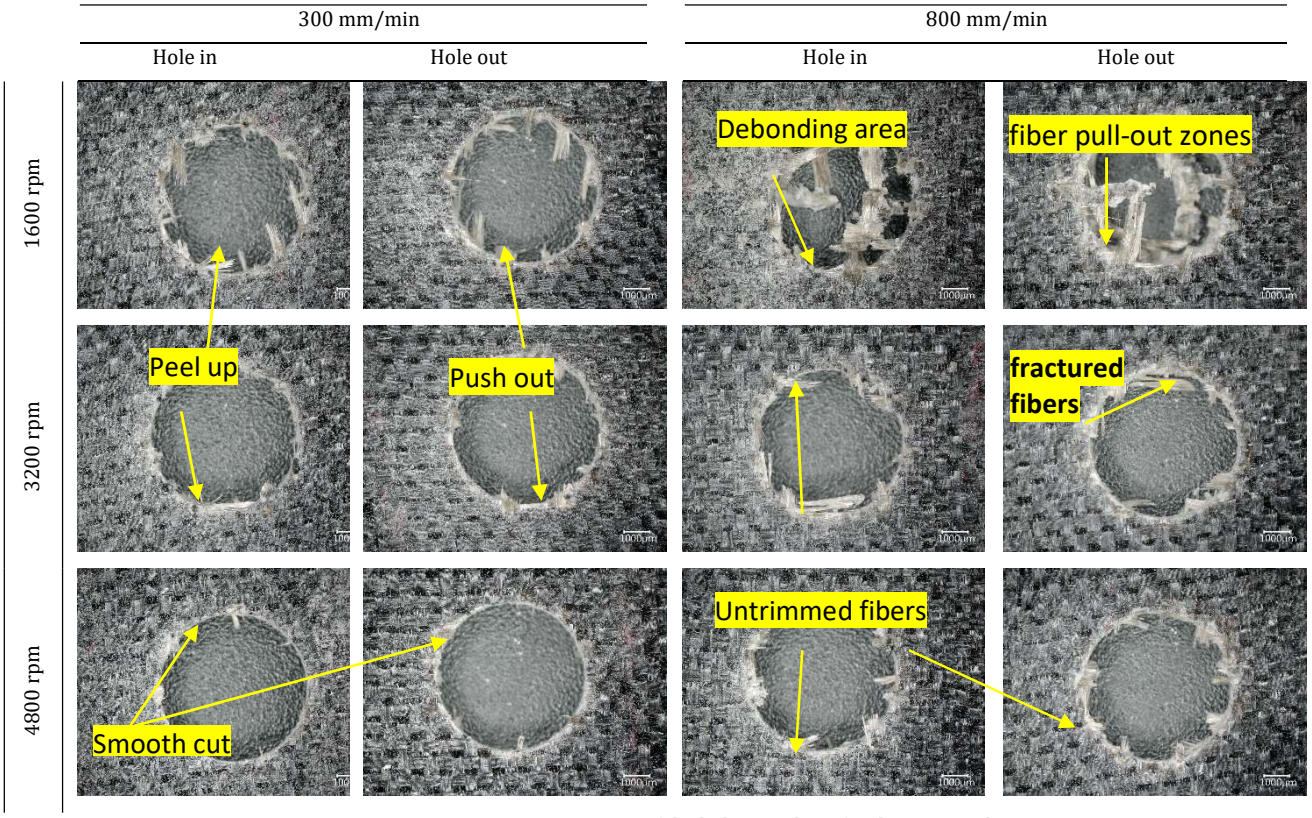


Figure 11. Microscope images of the hole in and out for the N2 sample

| | 300 mm/min | | 800 mm/min | |
|---|---|---|---|---|
| | Hole in | Hole out | Hole in | Hole out |

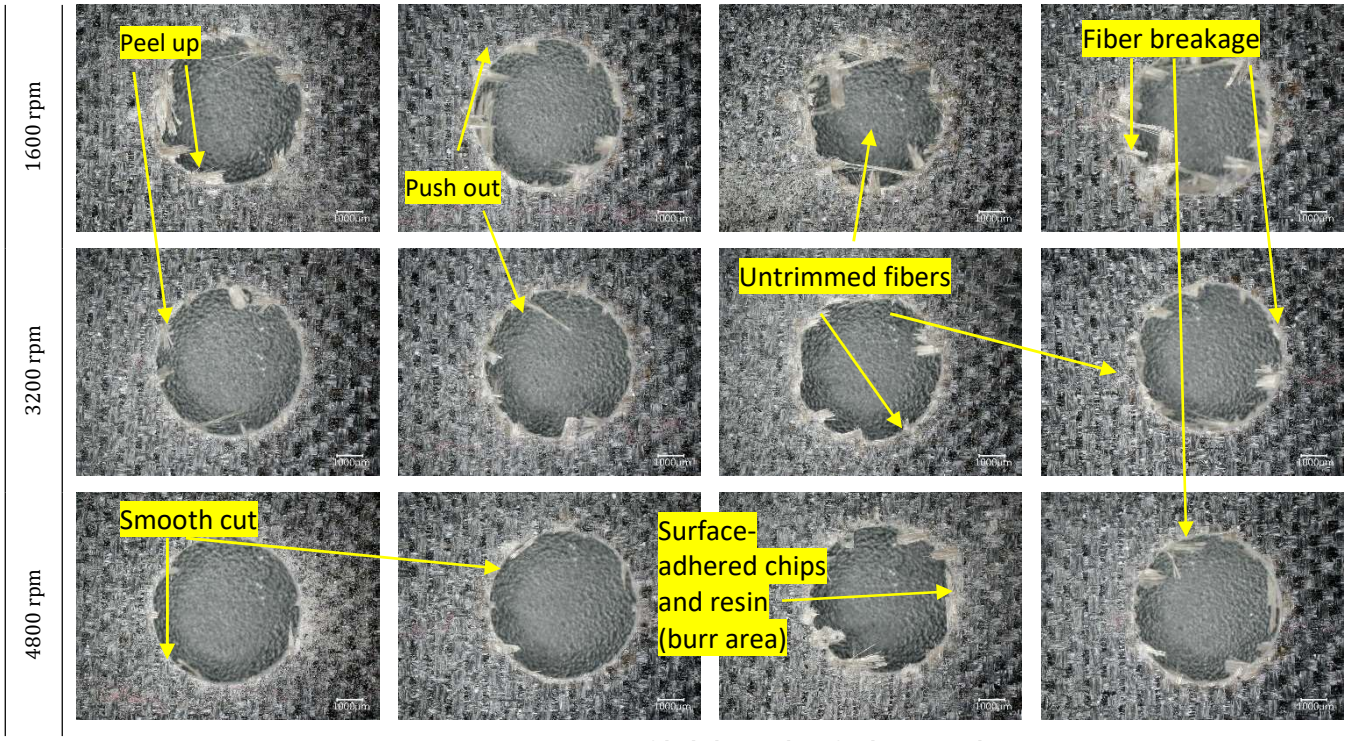


Figure 12. Microscope images of the hole in and out for the N3 sample

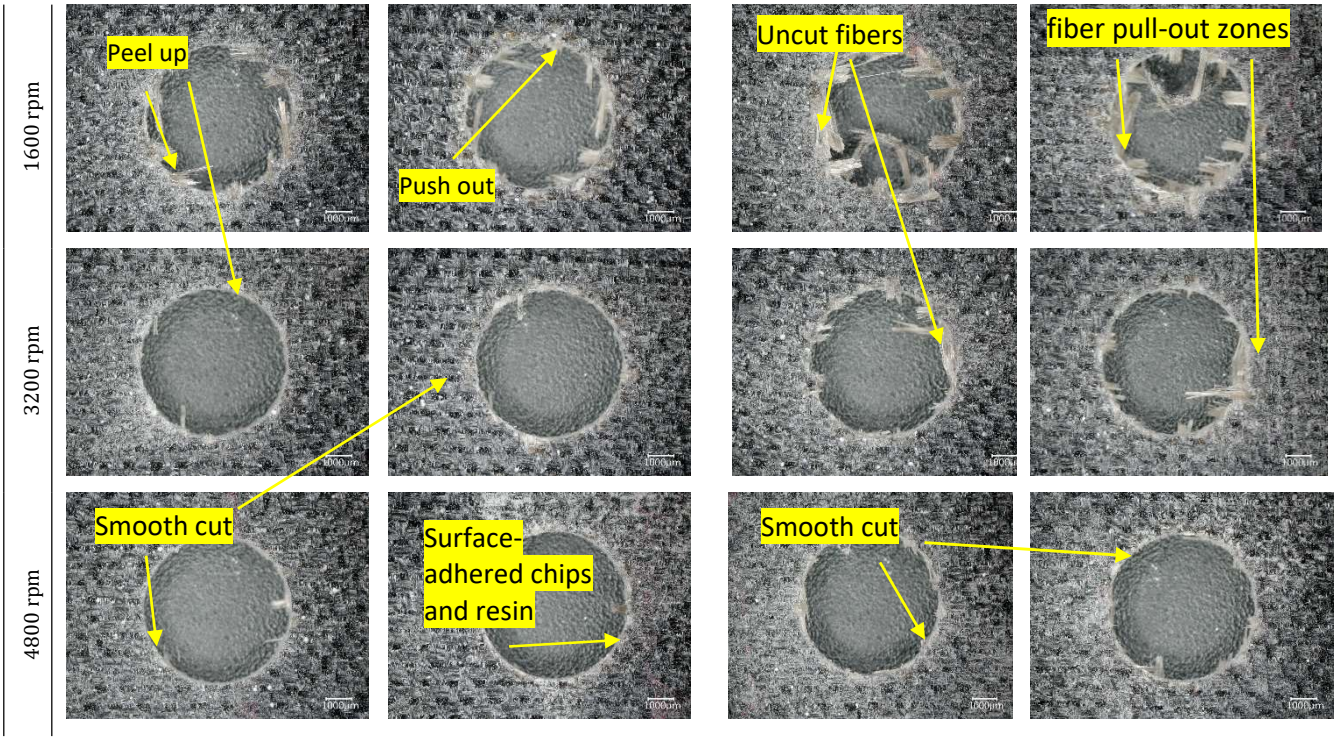


Figure 13. Microscope images of the hole in and out for the N4 sample

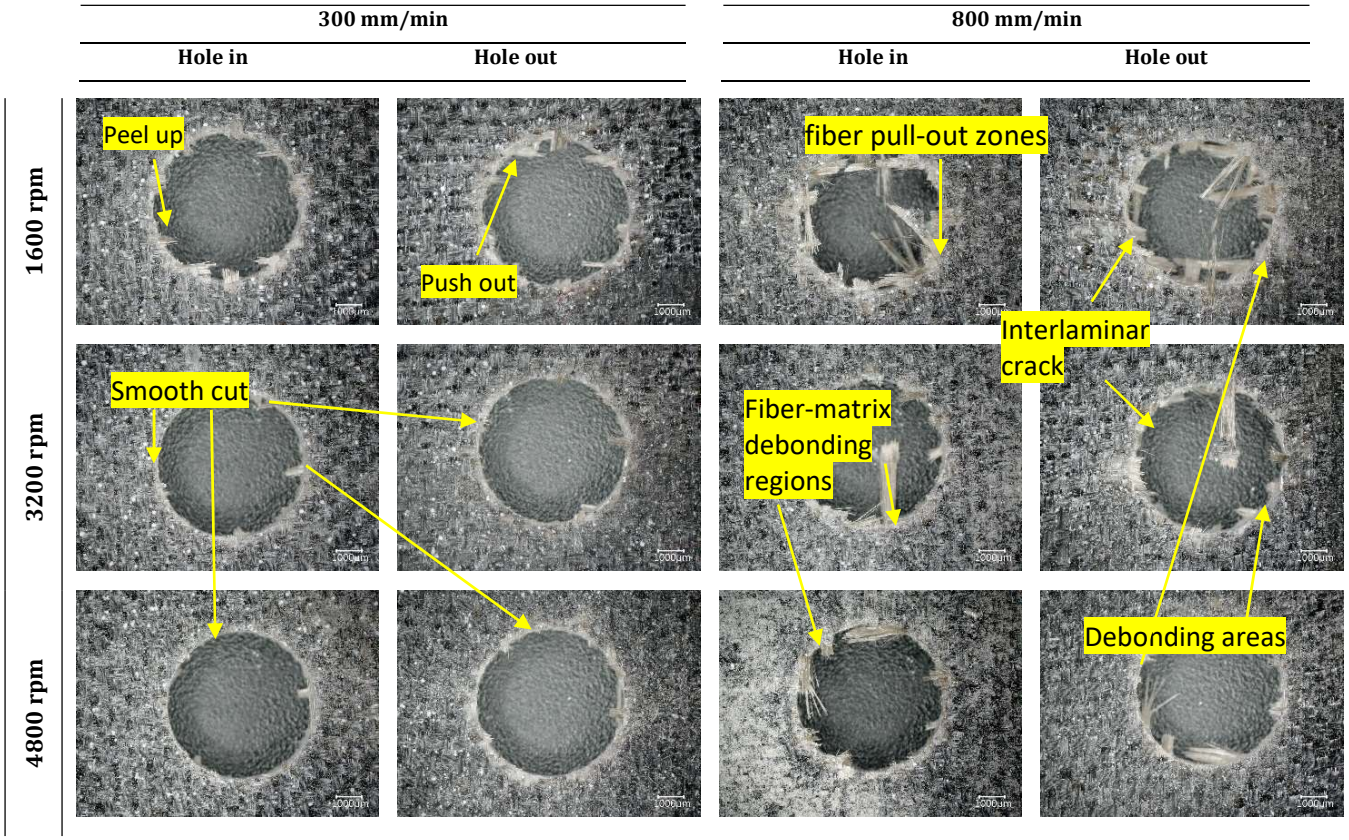


**Figure 1.** Microscope images of the hole in and out for the N5 sample

Table 4. Delamination factor values generated during the drilling process for all samples

| Feed Rate | Spindle speed | N0 sample | | N1 sample | | N2 sample | |
|---|---|---|---|---|---|---|---|
| | | $D_{fin}$ | $D_{fout}$ | $D_{fin}$ | $D_{fout}$ | $D_{fin}$ | $D_{fout}$ |
| 300 mm/min | 1600 rpm | 1.2349 | 1.2381 | 1.2342 | 1.1860 | 1.1648 | 1.1993 |
| | 3200 rpm | 1.1624 | 1.1854 | 1.1749 | 1.2028 | 1.1009 | 1.1778 |
| | 4800 rpm | 1.1296 | 1.2011 | 1.1548 | 1.1958 | 1.0870 | 1.1434 |
| 800 mm/min | 1600 rpm | 1.3121 | 1.2367 | 1.2876 | 1.3490 | 1.1386 | 1.2260 |
| | 3200 rpm | 1.2437 | 1.1581 | 1.2356 | 1.1909 | 1.1131 | 1.1145 |
| | 4800 rpm | 1.2032 | 1.2066 | 1.1797 | 1.2213 | 1.1125 | 1.1161 |
| **Feed Rate** | **Spindle speed** | **N3 sample** | | **N4 sample** | | **N5 sample** | |
| | | $D_{fin}$ | $D_{fout}$ | $D_{fin}$ | $D_{fout}$ | $D_{fin}$ | $D_{fout}$ |
| 300 mm/min | 1600 rpm | 1.1538 | 1.1468 | 1.0967 | 1.1849 | 1.1448 | 1.1815 |
| | 3200 rpm | 1.1350 | 1.1140 | 1.0896 | 1.1784 | 1.1333 | 1.1384 |
| | 4800 rpm | 1.0993 | 1.1354 | 1.0794 | 1.1293 | 1.1010 | 1.1133 |
| 800 mm/min | 1600 rpm | 1.1527 | 1.2484 | 1.1748 | 1.2296 | 1.1682 | 1.1321 |
| | 3200 rpm | 1.0826 | 1.1301 | 1.1337 | 1.1662 | 1.1515 | 1.1156 |
| | 4800 rpm | 1.1748 | 1.1314 | 1.1264 | 1.1287 | 1.1118 | 1.1137 |

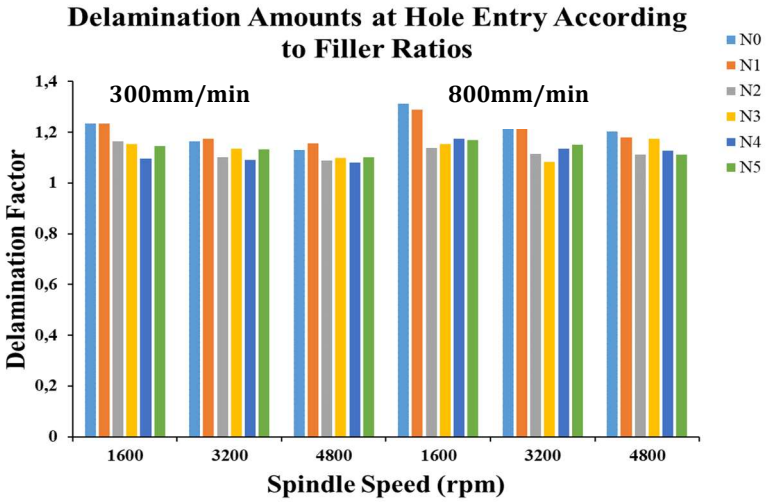


Figure 15. Delamination amounts at hole entry according to contribution ratios

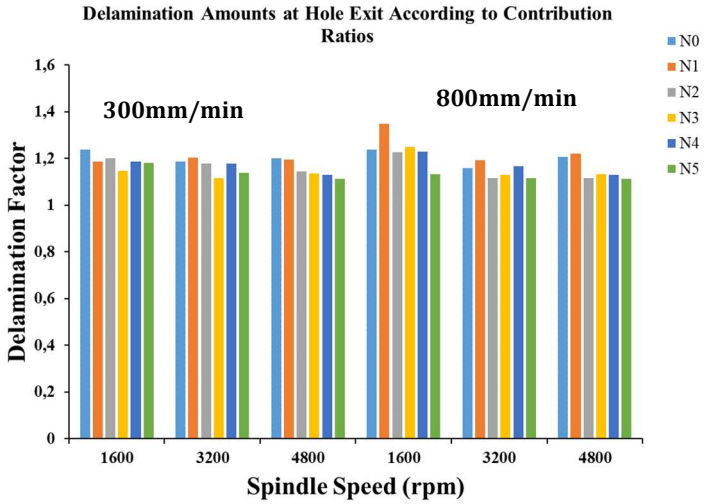


Figure 26. Delamination amounts at hole exit according to contribution ratios

Many studies have reported that drilling-induced delamination can affect the material strength, load-bearing capacity, service life, and machining quality. Therefore, it is important to perform delamination analysis after the drilling process. Delamination formation is typically associated with the thrust force [30]. The hole images of the unreinforced N0 sample were shown in Figure 9. Upon examining the images, it was observed that there was no delamination or cracking at low feed rates, and most of the drilling processes resulted in burr-free holes. However, as the feed increased, burr formation also increased. At low spindle speeds, as the feed rate increased, the drill bit could not effectively evacuate the chips from the material surface [24], resulting in burr formation around the hole. Delamination at the hole exit occurred in the form of a push-out, meaning that thrust force had a significant effect on this type of damage. On the other hand, since the delamination at the hole entrance occurred as a peel-up, the effect of the thrust force here was less [8-9]. The observed delamination effect was consistent with the tensile strength and thrust force. The hole images of the N1 sample were shown in Figure 10. With a 0.5% weight h-BN addition, the matrix (resin), which holds the fibers together and distributes the load uniformly across the fibers, appears to reduce delamination formation by supporting the fibers against interlayer separation due to the added nanoparticle [31]. In other words, with the nanoparticle addition, the lubricating effect of the h-BN nanoparticles not only enhanced the material's durability but also prevented excessive deformation, leading to better performance. The hole images of the N2 sample were shown in Figure 11. With a 0.25% weight of MWCNT, the fiber and matrix integrity of the composite material increased, significantly improving machinability. Upon detailed examination of the hole images, it was observed that the composite with no additives exhibited delamination in the form of cracking at the hole exit, whereas the composite material with the additive showed block-like delamination at the exit. The addition of MWCNT resulted in better chip removal and the desired hole size due to the rigid, non-flexible structure of the composite MWCNT material [32]. The hole images of the N3, N4, and N5 samples, prepared with 0.25% weight MWCNT and 0.25%, 0.50%, and 0.75% weight h-BN nanoparticle

ISSN: 2149-9373 

additions, were shown in Figure 12, Figure 13, Figure 14. As with all other sample, lower delamination values were achieved at low cutting speeds and high spindle speeds. The main reason for this is the increased friction at the tool edges at high spindle speeds and low cutting speeds. This results in the matrix softening, allowing the cutting process to occur more stably and reducing delamination errors [33-34]. It was observed that MWCNT significantly reduced delamination, but at higher concentrations of h-BN, this error increased again. Delamination is primarily controlled by the cutting mechanism during processing. Higher nanoparticle additions increase machinability up to a certain limit and, by reaching the minimum chip thickness, provide lower delamination and improved surface quality. The best delamination result was obtained with the dN3L1S3 sample. However, when this limit was exceeded, it was observed that increased peeling areas, separation, and interlayer cracks led to negative effects [27].

### 3.3. Test results for surface roughness analysis in drilling operation

The surface roughness values for the N0, N1, N2, N3, N4, and N5 composite samples at spindle speeds of 1600, 3200, and 4800 RPM, and feed rates of 300 and 800 mm/min, were presented in Figure 17 and Figure 18. It was observed that as the spindle speed increased, surface roughness decreased, while surface roughness increased with higher feed rates. The results also showed a linear relationship between cutting force and surface roughness.

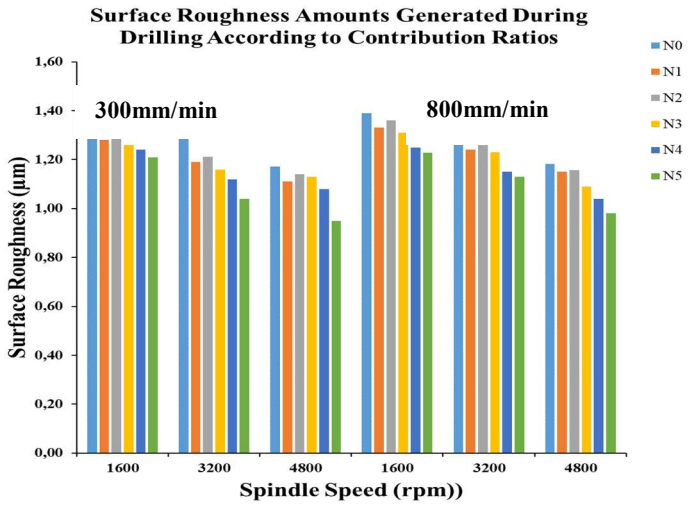


Figure 37.Surface Roughness Amounts Generated During Drilling According to Contribution Ratios

Table 5. Surface roughness values generated during the drilling process for all samples and percentage change rates for the N0 sample

| Feed Rate | Spindle speed | N0 sample Ra(µm) | N0 sample Percentage change rates (%) | N1 sample Ra(µm) | N1 sample Percentage change rates (%) | N2 sample Ra(µm) | N2 sample Percentage change rates (%) |
|---|---|---|---|---|---|---|---|
| 300 mm/min | 1600 rpm | 1.45 | - | 1.28 | -11.72 | 1.34 | -7.59 |
| | 3200 rpm | 1.32 | - | 1.19 | -9.85 | 1.21 | -8.26 |
| | 4800 rpm | 1.17 | - | 1.11 | -5.29 | 1.14 | -2.73 |
| 800 mm/min | 1600 rpm | 1.39 | - | 1.33 | -4.32 | 1.36 | -2.16 |
| | 3200 rpm | 1.29 | - | 1.24 | -3.80 | 1.26 | -2.25 |
| | 4800 rpm | 1.18 | - | 1.15 | -2.79 | 1.16 | -2.28 |

| Feed Rate | Spindle speed | N3 sample Ra(µm) | N3 sample Percentage change rates (%) | N4 sample Ra(µm) | N4 sample Percentage change rates (%) | N5 sample Ra(µm) | N5 sample Percentage change rates (%) |
|---|---|---|---|---|---|---|---|
| 300 mm/min | 1600 rpm | 1.26 | -13.10 | 1.24 | -14.48 | 1.21 | -16.55 |
| | 3200 rpm | 1.16 | -12.12 | 1.12 | -15.15 | 1.04 | -21.21 |
| | 4800 rpm | 1.13 | -3.58 | 1.08 | -7.85 | 0.95 | -18.94 |
| 800 mm/min | 1600 rpm | 1.31 | -5.76 | 1.25 | -10.07 | 1.23 | -11.65 |
| | 3200 rpm | 1.23 | -4.58 | 1.15 | -10.78 | 1.13 | -12.34 |
| | 4800 rpm | 1.09 | -7.86 | 1.04 | -12.09 | 0.98 | -17.16 |

When examining the surface roughness of the N1sample with 0.5% weight h-BN nanoparticle addition, it shows lower surface roughness values compared to the N0 sample without h-BN nanoparticles. This clearly indicates that the added nanoparticle reduces the likelihood of chips remaining in the newly machined area [35], in other words, it reduces friction due to its lubricating properties, thereby lowering surface roughness under certain processing conditions [36]. When the surface roughness of the N2 sample with 0.25% weight MWCNT nanoparticle addition is examined, a reduction in surface roughness is observed compared to the unreinforced N0 sample, although this reduction is less than that observed in the N1 sample. This suggests that the dense network structure of MWCNTs increases the surface roughness of the sample. High MWCNT concentrations in polymer composites lead to the locking of polymer chains, leaving slight marks on the cutting surface [37-38]. At the same time, surface quality is largely controlled by the cutting mechanism during processing; therefore, excessive amounts of MWCNT reinforcement in composites result in the MWCNTs, rather than the polymer, forming the cutting process [39]. As a result, in the N2 sample, a higher thrust force and surface roughness were obtained with the MWCNT addition compared to the N1 sample. By keeping the MWCNT content constant and increasing the h-BN content, lower surface roughness values were achieved in the N3, N4, and N5 samples compared to the N0 sample. As the h-BN content increased, similar to the thrust force, a decrease in surface roughness was observed.

## 4. Conclusion

The findings from the drilling operations were summarized as follows:

Thrust Force: As the feed rate increased, the thrust force increased, while an increase in spindle speed led to a decrease. The lowest thrust forces were obtained at a feed rate of 300 mm/min and spindle speed of 4800 rpm. In the h-BN added samples, a reduction of up to 6.72% in thrust force was observed, while this reduction was more limited in the MWCNT-based samples.

Delamination: No delamination or burr formation was observed at low feed rates, while burr formation increased with higher feed rates. The h-BN added samples reduced delamination, while the MWCNT added samples provided smoother and block-type delamination at the hole exit.

Surface Roughness: Surface roughness decreased with increasing spindle speed and increased with higher feed rates. The h-BN added samples exhibited lower surface roughness values. The lowest roughness value, 0.95 µm, was measured for the N5 sample.

These findings highlight the significant effects of optimizing processing parameters (feed rate, spindle speed) on thrust force, delamination, and surface roughness during the drilling process.

## Acknowledgment

This study was funded by the Scientific Research Projects Coordination Unit of Necmettin Erbakan University under project number 221451002.

## Conflict of Interest Statement

The authors declare that there is no conflict of interest

## References

[1] M. Kishore, M. Amrita, and B. Kamesh, "Experimental investigation of milling on basalt-jute hybrid composites with graphene as nanofiller," *Materials Today: Proceedings*, vol. 43, pp. 726–730, Jan. 2021. doi: 10.1016/j.matpr.2020.12.847

[2] K. K. Chawla, *Composite materials: Science and engineering*, third edition, New York: Springer, 2012. doi: 10.1007/978-0-387-74365-3

[3] D. Matykiewicz, M. Barczewski, D. Knapski, and K. Skórczewska, "Hybrid effects of basalt fibers and basalt powder on thermomechanical properties of epoxy composites," *Composites Part B: Engineering*, vol. 125, pp. 157–164, Sep. 2017. doi: 10.1016/j.compositesb.2017.05.060

[4] K. El-Ghaoui, J. F. Chatelain, and C. Ouellet-Plamondon, "Effect of Graphene on Machinability of Glass Fiber Reinforced Polymer (GFRP)," *Journal of Manufacturing and Materials Processing*, vol. 3, no. 3, p. 78, Sep. 2019. doi: 10.3390/jmmp3030078

[5] Y. H. Çelik, E. Kilickap, and A. İ. Kilickap, "An experimental study on milling of natural fiber (jute)- reinforced polymer composites," *Journal of Composite Materials*, vol. 53, no. 22, pp. 3127–3137, Sep. 2019. doi: 10.1177/0021998319826373

 

[6] F. Javanshour et al., "Effect of graphene oxide surface treatment on the interfacial adhesion and the tensile performance of flax epoxy composites," *Composites Part A: Applied Science and Manufacturing*, vol. 142, p. 106270, Mar. 2021. doi: 10.1016/j.compositesa.2020.106270

[7] F. B. Gumus, F. Ceritbinmez, and A. Yapici, "The effect of hexagonal nano boron nitride on mechanical performances and machinability behaviors of basalt fabric reinforced epoxy composites," *Proceedings of Materials Science and Engineering*, vol. 235, no. 23, pp. 7161–7168, May 2021. doi: 10.1177/09544062211013374

[8] S. Morkavuk, K. Aslantaş, L. Gemi, U. Köklü, and Ş. Yazman, "The influence of drilling-induced damages and hole quality on hoop tensile and fatigue behavior of CFRP tubes," *Composites Part A: Applied Science and Manufacturing*, vol. 179, p. 108005, Apr. 2024. doi: 10.1016/j.compositesa.2024.108005

[9] Ş. Yazman, L. Gemi, S. Morkavuk, and U. Köklü, "Investigation of the effect of symmetrical hybrid stacking on drilling machinability of unidirectional CFRP, GFRP and hybrid composites: Drilling tests and damage analysis," *Composites Part A: Applied Science and Manufacturing*, vol. 187, p. 108486, Dec. 2024. doi: 10.1016/j.compositesa.2024.108486

[10] F. Turan, "The effect of MWCNT concentration on the electrical resistance change characteristic of glass/fiber epoxy composites under low cycle fatigue loading," *Materials Testing*, vol. 67, no. 1, pp. 1–16, Jan. 2025. doi: 10.1515/mt-2024-0107

[11] N. Geier, J. P. Davim, and T. Szalay, "Advanced cutting tools and technologies for drilling carbon fibre reinforced polymer (CFRP) composites: A review," *Composites Part A: Applied Science and Manufacturing*, vol. 125, p. 105552, Oct. 2019. doi: 10.1016/j.compositesa.2019.105552

[12] S. Margabandu and S. Subramaniam, "An experimental investigation of thrust force, delamination and surface roughness in drilling of jute/carbon hybrid composites," *World Journal of Engineering*, vol. 17, no. 5, pp. 661–674, Jul. 2020. doi: 10.1108/WJE-03-2020-0080

[13] T. Gao et al., "Carbon fiber reinforced polymer in drilling: From damage mechanisms to suppression," *Composite Structures*, vol. 286, p. 115232, Apr. 2022. doi: 10.1016/j.compstruct.2022.115232

[14] N. Deshpande, H. Vasudevan, and R. Rajguru, "Experimental investigation and optimization of milling parameters in the machining of NEMA G-11 GFRP composite material using PCD tool," in *Proc. 5th International and 26th All India Manufacturing Technology, Design and Research Conference (AIMTDR 2014)*, Guwahati, India, Dec. 2014, pp. 2105–2114.

[15] M. Ramesh and A. Gopinath, "Measurement and analysis of thrust force in drilling sisal-glass fiber reinforced polymer composites," in *IOP Conference Series: Materials Science and Engineering*, vol. 197, May 2017, p. 012056. doi: 10.1088/1757-899X/197/1/012056

[16] H. Ejaz, A. Mubashar, M. A. M, and S. Waqar, "Effect of GNP and MWCNT Addition on Lap Shear Strength of Adhesively Bonded Joints," in *2022 19th International Bhurban Conference on Applied Sciences and Technology*, Islamabad, Pakistan, Aug. 15–17, 2022, pp. 116–121. Piscataway, NJ: IEEE, 2022. doi: 10.1109/IBCAST54850.2022.9990107

[17] Ş. Yazman, "Investigation of the Mechanical Properties of Hybrid Nanocomposite Adhesives Reinforced with Carbon Nanotube and Ceramic Nanoparticles," Ph.D. dissertation, Institute of Science, Necmettin Erbakan University, Konya, Turkey, 2018.

[18] M. Tongur, "Experimental Investigation of the Mechanical and Thermal Properties of Nanoparticle-Modified Polyurethane Adhesives," M.Sc. thesis, Department of Mechanical Engineering, Institute of Science, Necmettin Erbakan University, Konya, Turkey, 2020.

[19] G. Bahtiyar, M. Ekrem, B. Ünal, and S. Ak, "Mechanical Properties and Damage Behaviours of Polyurethane Composites Reinforced With BNNP and MWCNT Hybrid Nanoparticles," *Journal of Elastomers and Plastics*, vol. 55, no. 4, pp. 613–625, Mar. 2023. doi: 10.1177/00952443231165427

[20] P. KumarKharwar, R. KumarVerma, and A. Singh, "Simultaneous optimisation of quality and productivity characteristics during machining of multiwall carbon nanotube/epoxy nanocomposites," 2020. doi: 10.1080/14484846.2020.1794511

[21] S. Morkavuk, "Investigation of the Effect of Drilling Process on the Mechanical and Fatigue Behavior of Carbon Fiber Reinforced Composite Tubes," Ph.D. dissertation, Afyon Kocatepe University, Afyon, Turkey, 2023.

[22] Y. H. Çelik, E. Kilickap, and N. Koçyiğit, "Evaluation of drilling performances of nanocomposites reinforced with graphene and graphene oxide," *International Journal of Advanced Manufacturing Technology*, vol. 100, no. 9, pp. 2371–2385, 2018. doi: 10.1007/s00170-018-2875-Z

[23] U. A. Khashaba, "A novel approach for characterization of delamination and burr areas in drilling FRP composites," *Composite Structures*, vol. 290, p. 115534, Jun. 2022. doi: 10.1016/j.compstruct.2022.115534

[24] H. B. Upputuri and V. S. Nimmagadda, "Optimization of drilling process parameters used in machining of glass fiber reinforced epoxy composite," *Materials Today: Proceedings*, vol. 23, pp. 594–599, 2020. doi: 10.1016/j.matpr.2019.05.415

[25] A. Can, "Study on the machinability of SMC composites during hole milling: Influence of tool geometry and machining parameters," *Arabian Journal for Science and Engineering*, vol. 44, no. 4, pp. 7599–7616, Apr. 2019. [Online]. Available: https://link.springer.com/article/10.1007/s13369-019-03865-z. [Accessed: 25-Jun-2025]

[26] K. K. Panchagnula and K. Palaniyandi, "Drilling on fiber reinforced polymer/nanopolymer composite laminates: a review," *Journal of Materials Research and Technology*, vol. 7, no. 2, pp. 180–189, 2018. doi: 10.1016/j.jmrt.2017.06.003

[27] K. Xiao and L. Zhang, "The role of viscous deformation in the machining of polymers," *International Journal of Mechanical Sciences*, vol. 44, no. 11, pp. 2317–2336, Nov. 2002. doi: 10.1016/S0020-7403(02)00178-9

[28] J. Samuel, A. Dikshit, R. E. DeVor, S. G. Kapoor, and K. J. Hsia, "Effect of Carbon Nanotube (CNT) Loading on the Thermomechanical Properties and the Machinability of CNT-Reinforced Polymer Composites," *Journal of Manufacturing Science and Engineering*, vol. 131, no. 3, Jun. 2009. doi: 10.1115/1.3123337

[29] S. Madarvoni and R. P. S. Sreekanth, "Mechanical Characterization of Graphene—Hexagonal Boron Nitride-Based Kevlar–Carbon Hybrid Fabric Nanocomposites," *Polymers (Basel)*, vol. 14, no. 13, 2022. doi: 10.3390/polym14132559

[30] D. Geng, X. Chen, L. Fang, ve H. Wang, "Delamination formation, evaluation and suppression during drilling of composite laminates: A review," *Composite Structures*, vol. 216, pp. 168–186, May 2019. doi: 10.1016/j.compstruct.2019.02.099

[31] C. Guo, H. Zhang, ve Y. Wang, "Mechanical and thermal properties of multiwalled carbon-nanotube-reinforced $Al_2O_3$ nanocomposites," *Ceramics International*, cilt. 46, ss. 17,449–17,460, 2020. doi: 10.1016/j.ceramint.2020.04.039

[32] Z. Li, J. Ma, H. Ma, and X. Xu, "Properties and Applications of Basalt Fiber and Its Composites," in *IOP Conference Series: Earth and Environmental Science*, Institute of Physics Publishing, Oct. 2018. doi: 10.1088/1755-1315/186/2/012052

[33] V. N. Gaitonde, S. R. Karnik, J. C. Rubio, A. E. Correia, A. M. Abrão, and J. P. Davim, "Analysis of parametric influence on delamination in high-speed drilling of carbon fiber reinforced plastic composites," *Journal of Materials Processing Technology*, vol. 203, no. 1–3, 2008. doi: 10.1016/j.jmatprotec.2007.10.050

[34] S. R. Karnik, V. N. Gaitonde, J. C. Rubio, A. E. Correia, A. M. Abrão, and J. P. Davim, "Delamination analysis in high speed drilling of carbon fiber reinforced plastics (CFRP) using artificial neural network model," *Materials & Design*, vol. 29, no. 9, pp. 1768–1776, 2008. doi: 10.1016/j.matdes.2008.03.014

[35] A. A. Abdul Nasir, A. I. Azmi, and A. N. M. Khalil, "Measurement and optimisation of residual tensile strength and delamination damage of drilled flax fibre reinforced composites," *Measurement*, vol. 75, 2015. doi: 10.1016/j.measurement.2015.07.046

[36] K. R. Sumesh and K. Kanthavel, "Abrasive water jet machining of Sisal/Pineapple epoxy hybrid composites with the addition of various fly ash filler," *Materials Research Express*, vol. 7, no. 3, p. 035303, Mar. 2020. doi: 10.1088/2053-1591/ab7865

[37] K. Bhowmik, S. K. Basantia, T. Roy, A. Bandyopadhyay, N. Khutia, and A. R. Chowdhury, "Mechanical Properties of MWCNT Reinforced Epoxy Nanocomposites: Experimental, Micromechanical and Numerical Study," *Journal of the Institution of Engineers (India): Series D*, vol. 103, no. 2, pp. 575–586, Dec. 2022. doi: 10.1007/s40033-022-00358-6

[38] R. Farshbaf Zinati, M. R. Razfar, and H. Nazockdast, "Surface Integrity Investigation for Milling PA 6/MWCNT," *Materials and Manufacturing Processes*, vol. 30, no. 8, pp. 1035–1041, Aug. 2015. doi: 10.1080/10426914.2014.961473

[39] R. K. Verma, V. K. Singh, D. K. Singh, and P. K. Kharwar, "Experimental investigation on surface roughness and circularity error during drilling of polymer nanocomposites," *Materials Today: Proceedings*, vol. 44, pp. 2501–2506, 2021. doi: 10.1016/j.matpr.2020.12.597